Dendritic cell NLRC4 regulates influenza A virus-specific CD4 T cell responses through FasL expression
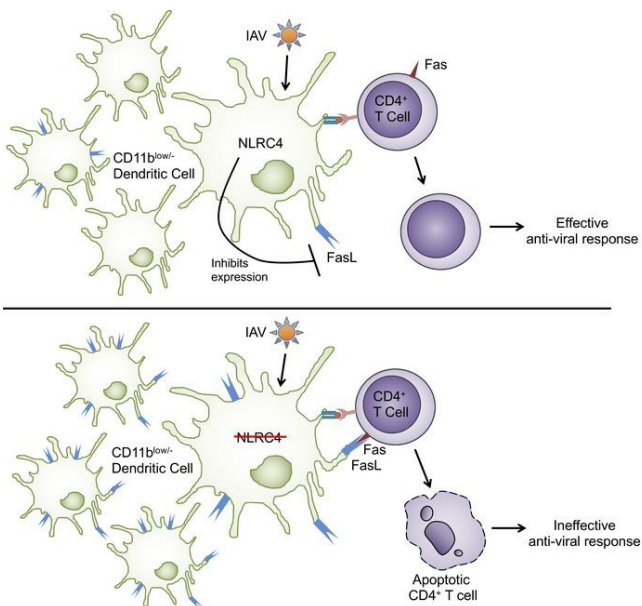
Emma E. Hornick, … , Fayyaz S. Sutterwala, Suzanne L. Cassel

Research | In-Press Preview | Immunology | Virology

Graphical abstract

Dendritic cell NLRC4 regulates influenza A virus-specific CD4 T cell responses through FasL expression

Emma E. Hornick,[1] Jargalsaikhan Dagvadorj,[2,3] Zeb R. Zacharias,[1,4] Ann M. Miller,[5] Ryan A. Langlois,[6] Peter Chen,[2,3] Kevin L. Legge,[1,4,7] Gail A. Bishop,[1,7,8,9] Fayyaz S. Sutterwala,[1,2,3,*] and Suzanne L. Cassel,[1,2,3,*]

[1]Interdisciplinary Program in Immunology, University of Iowa Carver College of Medicine, Iowa City, IA; [2]Department of Medicine, Cedars-Sinai Medical Center, Los Angeles, CA; [3]Women's Guild Lung Institute, Cedars-Sinai Medical Center, Los Angeles, CA; [4]Department of Pathology, University of Iowa Carver College of Medicine, Iowa City, IA; [5]Department of Surgery, University of Iowa Carver College of Medicine, Iowa City, IA; [6]Center for Immunology, University of Minnesota, Minneapolis, MN; [7]Department of Microbiology and Immunology, University of Iowa Carver College of Medicine, Iowa City, IA; [8]Department of Internal Medicine, University of Iowa Carver College of Medicine, Iowa City, IA; [9]Veterans Affairs Medical Center, Iowa City, IA.

*These authors contributed equally to this work

Key words: NLRC4, Inflammasome, FasL, Influenza virus, Dendritic cells

Short title: Protective role for Nlrc4 in influenza A virus infection

Correspondence to: Fayyaz Sutterwala, Cedars-Sinai Medical Center, 127 S. San Vicente Blvd, AHSP, Room A9402, Los Angeles, CA 90048; tel: (310) 423-2948; e-mail: fayyaz.sutterwala@cshs.org; or to Suzanne Cassel, Cedars-Sinai Medical Center, 127 S. San Vicente Blvd, AHSP, Room A9402, Los Angeles, CA 90048; tel: (310) 423-2948; e-mail: suzanne.cassel@cshs.org

Abstract

Influenza A virus (IAV)-specific T cell responses are important correlates of protection during primary and subsequent infections. Generation and maintenance of robust IAV-specific T cell responses relies on T cell interactions with dendritic cells (DCs). In this study, we explore the role of nucleotide-binding domain leucine-rich repeat containing receptor family member NLRC4 in modulating the DC phenotype during IAV infection. $Nlrc4^{-/-}$ mice had worsened survival and increased viral titers during infection, normal innate immune cell recruitment and IAV-specific CD8 T cell responses, but severely blunted IAV-specific CD4 T cell responses compared to wild-type mice. The defect in the pulmonary IAV-specific CD4 T cell response was not a result of defective priming or migration of these cells in $Nlrc4^{-/-}$ mice but was instead due to an increase in FasL$^+$ DCs, resulting in IAV-specific CD4 T cell death. Together, our data support a novel role for NLRC4 in regulating the phenotype of lung DCs during a respiratory viral infection, and thereby influencing the magnitude of protective T cell responses.

Introduction

Influenza A virus (IAV) is a respiratory pathogen responsible for seasonal epidemics that can cause severe disease and death, most commonly in the very young, very old, and immunocompromised portions of the population (1). Vaccination strategies have traditionally prioritized antibody responses, but there is increasing evidence that IAV-specific T cells confer heterosubtypic protection that correlates with reduced symptom severity during infection (2, 3). During a primary IAV infection, CD8 T cells are critical for viral clearance, which they accomplish by directly killing infected cells through death receptor interactions and perforin/granzyme (4, 5). IAV-specific CD4 T cells provide help to both the CD8 T cell and B cell responses and support the antiviral functions of innate immune cells through production of IFNγ (6). IAV-specific T helper 1 (Th1) cells comprise the majority of the IAV-specific CD4 T cell response, including the recently described cytotoxic CD4 T cells that directly kill IAV-infected cells (7). IAV-specific regulatory T cells (Tregs) are also present and help to restrain tissue damage caused by exaggerated non-specific innate immune responses and targeted cytotoxic CD8 T cell-mediated killing of infected cells (8-11).

Antigen-presenting cells (APCs) at the site of infection are indispensable for regulating the magnitude and character of T cell responses in diverse inflammatory contexts (12). Depletion of phagocytic cells in the lungs following IAV infection results in premature apoptosis of IAV-specific T cells, due to the loss of critical survival signals normally provided by dendritic cells (DCs) (13, 14). DC interactions with T cells can also result in T cell death, which is exemplified by enhanced killing of IAV-specific CD8 T cells by plasmacytoid DCs in the lung-draining lymph nodes (dLNs) during lethal IAV infection (15-17). Induction of the appropriate phenotype in DCs depends on receipt of pro-inflammatory signals through cytokine/chemokine receptors and pattern recognition receptors (PRRs).

NLRC4 is an intracellular PRR belonging to the nucleotide oligomerization and binding domain and leucine rich repeat-containing (NLR) family. NLRC4 is best described for its role as part of the multiprotein inflammasome complex that mediates processing and secretion of IL-1β and IL-18 and induces a pyroptotic

cell death (18). The NLRC4 inflammasome is activated in response to infection with Gram-negative bacteria, and the resultant IL-18 production in CD8α$^+$ DCs during infection is important for memory CD8 T cell activation in this context (19). NLRC4-deficient mice have also been reported to have defective intra-tumoral CD4 and CD8 T cell responses and increased tumor burdens in a syngeneic subcutaneous melanoma model (20). Considering the importance of T cell responses in viral infection and the evidence supporting a role for NLRC4 in direct or indirect modulation of T cell responses in these different settings, we assessed the role of NLRC4 in the host response to IAV infection. We report that *Nlrc4*$^{-/-}$ mice had decreased survival following IAV infection with an associated defective IAV-specific CD4 T cell response. The reduction in the CD4 T cell response in *Nlrc4*$^{-/-}$ mice was due to T cell extrinsic signals that result in increased death of IAV-specific CD4 T cells. We further showed that there was an increase in FasL$^+$ DCs in the lungs of IAV-infected *Nlrc4*$^{-/-}$ mice, and that blocking Fas-FasL interactions *in vitro* prevented CD4 T cell killing by NLRC4-deficient DCs. Finally, transfer of NLRC4-deficient DCs into WT mice conveyed both the increased mortality and the loss of CD4 T cells following IAV infection seen in *Nlrc4-/-* mice. Together our findings demonstrate a novel and critical role for NLRC4 in regulating IAV-specific CD4 T cell responses through FasL expression on DCs.

Results

Nlrc4$^{-/-}$ *mice have increased morbidity and mortality during IAV infection*

To determine the effect of NLRC4 deficiency on outcome during IAV infection, we compared the morbidity and mortality of wild-type (WT) and *Nlrc4*$^{-/-}$ mice following infection with IAV. We observed significantly increased morbidity and mortality among the *Nlrc4*$^{-/-}$ animals compared to WT animals (Figure 1A and B), accompanied by increased viral titers in the lungs of *Nlrc4*$^{-/-}$ mice at 1, 3, and 7 days post-infection (Figure 1C). Susceptibility of *Nlrc4*$^{-/-}$ mice to IAV was dose dependent and infection with $0.25LD_{50}$ inoculum of IAV resulted in similar

mortality between WT and *Nlrc4*^{-/-} mice (Figure 1D). Consistent with previous studies *Asc*^{-/-} mice had increased mortality compared to WT (Figure 1D) (21, 22).

NLRC4 is best known for its role as part of the NLRC4 inflammasome, which is formed upon recognition of bacterial flagellin and components of the type III secretion system by Naip proteins (23, 24). Activation of the NLRC4 inflammasome results in cleavage of pro-caspase-1 into its active form, which in turn cleaves pro-IL-1β and pro-IL-18 to their mature secreted forms. Formation of the NLRC4 inflammasome within the lungs seemed unlikely in the context of a viral infection, and indeed we detected no defect in cleavage of pro-caspase-1 in lung homogenates from *Nlrc4*^{-/-} mice at 24 hrs post-infection with IAV (Figure 1E). These data suggest an inflammasome-independent role for NLRC4 in the control of IAV infection in vivo.

Nlrc4^{-/-} *mice have intact production of inflammatory mediators and innate immune cells in the lungs*

Excessive inflammation is a well-documented cause of pathology during IAV infection (25, 26). Given the increased IAV-induced mortality among *Nlrc4*^{-/-} mice, we compared the production of inflammatory mediators in the lungs of WT and *Nlrc4*^{-/-} mice following IAV infection and found no significant differences (Supplemental Figure 1). Consistent with the similarity in the levels of innate cell chemoattractants in WT and *Nlrc4*^{-/-} mice, the number of lung-infiltrating and lung-resident inflammatory cells was similar in WT and *Nlrc4*^{-/-} mice at days three and five post-infection (Figure 1F-J).

Defective pulmonary IAV-specific T cell responses in Nlrc4^{-/-} *mice*

The IAV-specific CD4 T cell response occurs primarily within the lungs and comprises a wide variety of specificities with a relatively small proportion of the cells specific for each antigen (27-29). While useful for the immune response, this breadth of specificities complicates measurement of the total response as the sum of all the individual antigen specific responses. Hence, we quantified the total IAV-specific CD4 T cell response using the surrogate markers CD49d and

CD11a (30), which are highly expressed on antigen-experienced cells and, in the context of IAV infection, reflect the cells that have been exposed to IAV-specific antigen (31). There was a significant decrease in the total and IAV-specific CD4 T cell response in the lungs of $Nlrc4^{-/-}$ mice compared to WT mice at day seven post-infection (Figure 2A and B). Interestingly, the decrease in IAV-specific CD4 T cells in $Nlrc4^{-/-}$ mice was not present at days three or five post-infection in the lungs, lung-draining lymph node (dLN) or spleens (Figure 2A and B, Supplemental Figure 2A-D). $Nlrc4^{+/-}$ and $Nlrc4^{+/+}$ littermates had similar numbers of pulmonary IAV-specific CD4 T cells suggesting that the $Nlrc4$ gene is haplosufficient (Supplemental Figure 2E and F).

The IAV-specific CD4 T cell response is predominantly a Th1-polarized response with a smaller number of IAV-specific regulatory T cells (Treg), which are protective during a primary infection (7, 32, 33). Consistent with the significantly decreased number of total IAV-specific CD4 T cells in $Nlrc4^{-/-}$ mice, we found significant decreases in IAV-specific Th1 (Tbet$^+$) and Treg (Foxp3$^+$) cells (Figure 2C and D).

The IAV-specific CD8 T cell response is crucial for viral clearance during a primary IAV infection, thus we quantified this response in WT and $Nlrc4^{-/-}$ mice (34). There were small decreases in the frequency and number of total lung CD8 T cells that did not rise to the level of statistical significance (Figure 2E), and no significant difference in the frequency and number of total antigen-experienced CD8 T cells in the lungs was observed (Figure 2F).

Together, these data reveal a defect in the pulmonary IAV-specific CD4 T cell response in $Nlrc4^{-/-}$ mice. IAV-specific CD4 T cell responses are important for successful viral clearance and recovery from IAV infection (32, 35), thus these defects likely contribute to the enhanced mortality evident in $Nlrc4^{-/-}$ mice.

DC and T cell accumulation in lung draining lymph nodes is intact in $Nlrc4^{-/-}$ mice

To identify the cause of the blunted IAV-specific CD4 T cell response, we evaluated key steps in the generation of this response. Initiation of robust IAV-specific T cell responses relies on successful interactions in the secondary

lymphoid organs with antigen-bearing APCs, many of which have migrated from the lungs (6). Accelerated respiratory DC migration to the lung dLN lasts for about 48 hrs after IAV infection (36). At 24 hrs after infection, there was no significant difference in the proportion of CD11c$^+$ cells originating from the lungs in the lung dLN of WT and *Nlrc4$^{-/-}$* mice (Supplemental Figure 3A and B), indicating that defective DC migration was unlikely to be contributing to the blunted IAV-specific CD4 T cell response in *Nlrc4$^{-/-}$* mice. Further characterization of DC phenotype in the lung dLN revealed no differences in the abundance or expression of co-stimulatory molecules on DCs in WT and *Nlrc4$^{-/-}$* mice (Supplemental Figure 3C-H). These findings are consistent with the normal accumulation of total and antigen-experienced CD4 T cells in the lung dLN at three, and five days post-infection (Supplemental Figure 2C and D). Considered together, these data argue that a defect in activation and expansion of T cells in the dLN or spleen was not the cause of the blunted CD4 T cell response in the lungs of *Nlrc4$^{-/-}$* mice.

Increased T cell death in the lungs of Nlrc4$^{-/-}$ mice following IAV infection

Given that early DC-dependent events in the development of the IAV-specific CD4 T cell response appeared to proceed normally in *Nlrc4$^{-/-}$* mice, we assessed whether the decrease in CD4 T cells was due to increased death among these cells. Annexin V and viability staining showed increased dead or dying IAV-specific CD4 T cells in the lungs of *Nlrc4$^{-/-}$* mice compared to WT mice (Figure 3A). Consistently, IAV-specific CD4 T cells from the lungs of *Nlrc4$^{-/-}$* mice had more active Caspase-3/7 and active Caspase-8 as measured with a fluorescent inhibitor probe at seven days post-infection compared to CD4 T cells from WT mice (Figure 3B and C). These data suggest that increased death among IAV-specific CD4 T cells may be driving their diminished presence in *Nlrc4$^{-/-}$* lungs.

Increased IAV-specific CD4 T cell death in Nlrc4⁻/⁻ mice is T cell extrinsic

To determine whether the cause of death in *Nlrc4*$^{-/-}$ T cells was a defect intrinsic or extrinsic to the *Nlrc4*$^{-/-}$ T cells themselves, we set up a side-by-side comparison of WT and *Nlrc4*$^{-/-}$ T cells in WT and *Nlrc4*$^{-/-}$ hosts. We adoptively transferred both WT (CD90.1/2^{+}) and *Nlrc4*$^{-/-}$ (CD90.1^{+}) OT-II CD4 T cells, specific for the amino acids 323-339 of chicken ovalbumin (Ova$_{323-339}$), intravenously into WT and *Nlrc4*$^{-/-}$ recipients (CD90.2^{+}). One day later, we infected mice with IAV expressing the Ova$_{323-339}$ epitope and quantified the IAV-specific CD4 T cell response in the lungs at seven days post-infection. There were significantly more OT-II cells with an antigen-experienced phenotype in the lungs of WT hosts compared to *Nlrc4*$^{-/-}$ hosts, regardless of the OT-II donor genotype (Figure 3D), indicating that the cause of T cell death in the *Nlrc4*$^{-/-}$ mice is T cell extrinsic.

Increased FasL⁺ DCs in IAV-infected Nlrc4⁻/⁻ lungs

Blunting of T cell responses by FasL^{+} DCs occurs in diverse inflammatory contexts (15, 16, 37, 38), thus we explored DC-expression of FasL as a possible cause of the increased T cell death. We found that there were more FasL^{+} DCs (Siglec F^{-}CD11c^{+}) cells in the lungs, but not spleens, of *Nlrc4*$^{-/-}$ mice at seven days post-infection (Figure 4A, Supplemental Figure 4A, B) specifically within the CD11b^{low} and CD11b^{-} populations of DCs. The increase in FasL^{+} DCs matched the timing and location of the decrease in IAV-specific CD4 T cells, as there were no differences in FasL^{+} DCs at day five post-infection in the lungs of WT and *Nlrc4*$^{-/-}$ mice (Figure 4A, Supplemental Figure 4B). The geometric mean fluorescence intensity (GMFI) for FasL was not different between DCs from WT and *Nlrc4*$^{-/-}$ mice (Supplemental Figure 4C), consistent with more cells expressing FasL rather than higher expression per cell.

Consistent with the normal activation of caspase-1 in lungs from *Nlrc4*$^{-/-}$ mice following IAV infection, we observed no increase in FasL^{+} CD11b^{low} or FasL^{+} CD11b^{-} DCs in the lungs of *Caspase-1/11*$^{-/-}$ mice at seven days post-infection (Figure 4B, Supplemental Figure 5A). There was also no difference in

the proportion of Fas[+] IAV-specific CD4 T cells in the lungs of WT and *Nlrc4^{-/-}* mice, in agreement with the data indicating a T cell extrinsic cause of death (Supplemental Figure 5B).

To determine whether DCs from IAV-infected *Nlrc4^{-/-}* lungs were killing CD4 or CD8 T cells, we modified a previously described DC-T cell co-culture assay (15). At seven days post-infection, lung DCs and CD4 and CD8 T cells were isolated. Lung CD4 and CD8 T cell survival was measured following co-culture with isolated WT or *Nlrc4^{-/-}* CD11b^{hi}, CD11b^{low}, or CD11b^{-} lung DCs for 12 hours. Similar survival of CD4 T cells was observed following culture alone or following co-culture with *Nlrc4^{-/-}* and WT CD11b^{hi} DCs from the lungs, which had equivalent expression of FasL (Figure 5A). However, significantly fewer CD4 T cells survived culture with CD11b^{low} or CD11b^{-} lung DCs from *Nlrc4^{-/-}* mice, both of which contain more FasL^{+} cells than the corresponding DC populations from WT lungs (Figure 5A). Additionally, no difference in lung CD4 T cell survival was observed following co-culture with splenic DCs isolated from IAV-infected WT and *Nlrc4^{-/-}* mice, which have similar FasL expression (Supplemental Figure 5C). To test whether the increased killing of CD4 T cells by *Nlrc4^{-/-}* DCs was dependent on Fas-FasL interactions, we blocked this interaction by adding Fas-Fc to the co-cultures. Addition of Fas-Fc to co-cultures increased survival of IAV-specific lung CD4 T cells cultured with WT and *Nlrc4^{-/-}* lung DCs to similar levels (Figure 5A) but had no effect on CD4 T cells cultured alone (Supplemental Figure 5D), indicating that DC FasL is responsible for killing CD4 T cells. Consistent with the finding that CD8 T cell numbers in the lungs of IAV-infected mice were not significantly diminished in the absence of NLRC4 (Figure 2E, F), we observed similar survival of CD8 T cells following co-culture with *Nlrc4^{-/-}* and WT CD11b^{hi}, CD11b^{low}, or CD11b^{-} lung DCs (Figure 5B).

To confirm the enhanced IAV-induced mortality seen in *Nlrc4^{-/-}* mice was due to killing of CD4 T cells by FasL^{+} DCs, at five days post-infection WT mice received an intranasal transfer of WT or *Nlrc4^{-/-}* bone marrow-derived DCs (BMDC). Similar to CD11b^{low}CD11c^{+} and CD11b^{-}CD11c^{+} lung DCs (Figure 4A) we observed increased FasL expression on BMDC from *Nlrc4^{-/-}* mice

9

(Supplemental Figure 6A). While 40% of the WT mice that received WT BMDCs survived to post-infection day 14, WT mice that received $Nlrc4^{-/-}$ BMDCs had significantly greater mortality (Figure 5C). A subset of infected WT mice that received WT or $Nlrc4^{-/-}$ BMDCs had pulmonary CD4 and CD8 T cells enumerated on day seven post-infection. A marked loss of total and IAV-specific CD4 T cells in the WT hosts that received $Nlrc4^{-/-}$ BMDCs in comparison with the WT hosts treated with WT BMDCs was observed (Figure 5D and E, Supplemental Figure 6B, C). In contrast, no difference in IAV-specific CD8 T cells was observed in mice that received WT or $Nlrc4^{-/-}$ BMDCs (Figure 5F and G, Supplemental Figure 6D, E).

Decreased Akt1 and FoxO3a phosphorylation in NLRC4-deficient BMDCs

To determine how NLRC4 deficiency regulated FasL expression we examined the mRNA expression of *Fasl* in WT and $Nlrc4^{-/-}$ BMDCs by quantitative real-time PCR. $Nlrc4^{-/-}$ BMDCs expressed greater *Fasl* compared to WT BMDCs (Figure 6A). To confirm these findings, we assessed FasL on BMDCs from an independently generated $Nlrc4^{-/-}$ mouse line (39). We again observed increased FasL mRNA and protein in $Nlrc4^{-/-}$ BMDCs compared to WT (Supplemental Figure 6F and G). Consistent with inflammasome-independent regulation of FasL expression, we did not observe any significant difference in FasL expression in $Asc^{-/-}$ and $Caspase-1/11^{-/-}$ BMDCs compared to WT (Supplemental Figure 6H and I).

FoxO3a, a member of the Forkhead family of transcription factors, has been implicated in the regulation of FasL expression. Furthermore, phosphorylation of FoxO3a by the serine/threonine kinase Akt1 prevents FoxO3a-dependent transcription by inhibiting its translocation to the nucleus and preventing it from activating its target genes (40). BMDCs from $Nlrc4^{-/-}$ mice had diminished Akt1 and FoxO3a phosphorylation compared to WT BMDC (Figure 6B and C) suggesting that NLRC4 may regulate FasL expression through Akt1/FoxO3a phosphorylation.

Discussion

The data presented here show for the first time that *Nlrc4*^{-/-} mice have a defective immune response during IAV infection. *Nlrc4*^{-/-} mice show increased morbidity and mortality and impaired viral clearance, but these do not appear to be the result of a defect in cytokine/chemokine production or the innate immune response. Instead, we report a blunted IAV-specific CD4 T cell response in the lungs of *Nlrc4*^{-/-} mice. The number of pulmonary IAV-specific CD4 T cells is dramatically decreased, but CD8 T cells are largely unaffected. Ultimately, the loss of IAV-specific CD4 T cells in *Nlrc4*^{-/-} mice is a result of increased CD4 T cell death due to Fas-FasL-mediated killing by CD11b^{low} and CD11b^{-} DCs in the lungs.

The increased susceptibility of *Nlrc4*^{-/-} mice to IAV infection appears to be NLRC4 inflammasome-independent as we observed no changes in the inflammasome-dependent cytokines IL-1β or Caspase-1 cleavage in *Nlrc4*^{-/-} lungs during infection. The Nlrp3 and Aim2 inflammasomes are activated during IAV infection (21, 22, 41), thus the Caspase-1 activation and IL-1β secretion we observed are expected due to the activity of those inflammasomes. Interestingly, the level of IL-1β was slightly, but not significantly, increased in *Nlrc4*^{-/-} lungs by ELISA. This result may indicate increased activation of the Nlrp3 or Aim2 inflammasomes, which could be due to the elevated viral titers and therefore more abundant activating signals in *Nlrc4*^{-/-} mice.

Previous studies focused on the Nlrp3 inflammasome found no effect of NLRC4 deficiency on morbidity and mortality following IAV infection (21, 22). We find these data intriguing in light of the very clear survival defect in *Nlrc4*^{-/-} mice we report here. The reason for the differences in these studies is likely multifactorial. When we infected mice with a lower inoculum of IAV we no longer observed increased mortality of the *Nlrc4*^{-/-} mice compared to WT, however *Asc*^{-/-} mice were more susceptible even at this lower inoculum, consistent with the previously published findings (Figure 1D) (21, 22). Additionally, since those studies were published, we have developed an increased appreciation for the impact that genetic background has on knockout mice, and we postulate that

differences in the WT substrains used as controls and for backcrossing to $Nlrc4^{-/-}$ mice may further contribute. Of particular note, we and others have recently shown differences between C57BL/6J and C57BL/6N substrains in survival and inflammatory responses to IAV (31, 42). We and others have also reported striking differences in immune responses to additional inflammatory challenges between C57BL/6 substrains (42-44). In the present study, we have rigorously tested the specificity of our phenotype to a loss of NLRC4 through the use of littermate controls and confirmation in an independently generated $Nlrc4^{-/-}$ mouse (Supplemental Figure 2E, F, and 6F, G).

NLRC4 was recently reported by our laboratory to have an inflammasome-independent role in limiting melanoma progression (20). Although IAV infection and melanoma are considerably different challenges for the host immune system, in both cases a robust host T cell response is a correlate of protection. During both IAV infection and melanoma challenge, $Nlrc4^{-/-}$ mice exhibit defective T cell responses, and in both models myeloid cell dysfunction seems to be driving the defect (20). Intriguingly, it was recently shown that *FASLG* is highly expressed in a large number of human cancers, and that engineering tumor-specific T cells to resist Fas-mediated death is a promising strategy for enhancing immunotherapy during cancer (45). It would be of interest to determine whether there is NLRC4-mediated modulation of myeloid cell FasL during melanoma progression, and whether the ineffective melanoma-specific T cell responses observed in $Nlrc4^{-/-}$ mice could be rescued by disrupting Fas-FasL interactions or downstream signaling.

An important remaining question to answer is how NLRC4 is acting in these myeloid cells to influence FasL expression. Offering a single explanation that accounts for all of the observations is challenging because of the dynamic nature of immune responses and their regulatory mechanisms, but we speculate that NLRC4 may be involved in differentiation or activation of myeloid cells during an inflammatory insult. That unstimulated $Nlrc4^{-/-}$ BMDCs, but not $Casp1/11^{-/-}$ or $Asc^{-/-}$ BMDCs, have increased FasL mRNA and protein is suggestive of an inflammasome-independent function of NLRC4 in either the development and/or

differentiation of DCs. *Fasl* gene expression is controlled by a number of distinct transcription factor interactions at the *Fasl* promoter (46). FoxO3a can be phosphorylated by Akt1, resulting in its inactivation as a transcription factor. Conversely, dephosphorylation of FoxO3a results in upregulation of FasL and triggers increased apoptosis (40). In the absence of NLRC4 we observe diminished Akt1 and FoxO3a phosphorylation which may be driving increased FasL expression. As many signaling pathways involved in metabolism, cytokine sensing, and PAMP/DAMP sensing converge on AKT (47), it is possible that dysregulated activating signals in the absence of NLRC4 result in increased FasL expression.

In conclusion, the work described here demonstrates a protective role for NLRC4 during IAV infection. Protection is likely NLRC4 inflammasome-independent and involves supporting the IAV-specific CD4 T cell response in the IAV-infected lungs. In the absence of NLRC4, expression of FasL on CD11b^{low} and CD11b$^-$ lung DCs was increased, triggering more CD4 T cell death in the lungs of IAV-infected animals and associated increased mortality. These findings are of importance as they expand our understanding of how the IAV-specific CD4 T cell response in the lungs is regulated and implicate DC NLRC4 in the regulation of CD4 T cell responses.

Materials and Methods

Mice. The generation of *Nlrc4$^{-/-}$*, *Asc$^{-/-}$*, *Casp1/11$^{-/-}$* mice has been described elsewhere (48-50). Mice were backcrossed to C57BL/6N mice for at least ten generations and maintained in an SPF facility. C57BL/6N mice were purchased from the Charles River Laboratories and used as WT controls unless otherwise stated; B6.Cg-Tg(TcraTcrb)425Cbn/J (OT-II CD90.2$^+$) were purchased from Jackson Laboratories. Femurs from *Nlrc4$^{-/-}$* mice (39) were a gift from Dr. Matam Vijay-Kumar (University of Toledo, Toledo). Both male and female mice 6-12 weeks of age were used, however mice were sex-, age-, and weight-matched for individual experiments.

Virus and in vivo infection. Mouse-adapted IAV strain A/PR/8/34 (PR/8) was propagated as previously described (16). Recombinant IAV-OT-II was created using standard reverse genetics as previously described (51) and grown in 10 day-old embryonated chicken eggs (Charles River). The OT-II epitope (Ova$_{323-339}$) was inserted into the mRNA nucleotide position 186 encoding the neuraminidase stalk region, which is known to tolerate such insertions(52). Mice were anesthetized with ketamine and xylazine and infected intranasally with 0.5LD$_{50}$ virus diluted in 50µL sterile DMEM. Weight was monitored daily and mice were euthanized upon losing 30% of their starting weight. CFSE labeling of lung cells followed by IAV infection was performed as described (36), but CFSE was administered 15min prior to infection.

Lung titers. To measure virus titers, lungs were homogenized using a TissueTearor (Biospec), then homogenates were clarified by centrifugation and snap frozen in liquid nitrogen and stored at -80ºC. A standard plaque assay on MDCK cells was subsequently used to quantify infectious virus(53).

ELISA. Cytokines and chemokines were quantified in cell culture supernatants and lung homogenate supernatants using DuoSet mouse ELISA kits from R&D Systems: CXCL1, CXCL2, CXCL5, CXCL9, CXCL10, IL-1β, CCL2, CCL5; or ReadySetGo! mouse ELISA kits from eBioscience: IL-1α, IL-6, IL-10, TNFα following manufacturer's instructions.

Flow Cytometry. Single cell suspensions were prepared by pressing tissues through wire mesh screens (lungs) or dissociating between frosted ends of glass slides (spleens and lymph nodes). For some experiments, cells were minced and digested in Iscove's DMEM (Gibco) containing 1mg/mL collagenase XI (Sigma) and 0.02mg/mL DNase (Sigma) for 15 min at 37ºC prior to physical dissociation. Live cells were enumerated by Trypan blue exclusion. 1x10^6 cells per well of a 96-well plate (Corning) were blocked with 2% normal rat serum (Jackson laboratories) and anti-mouse CD16/32 (clone 2.4G2, Tonbo Biosciences) in

FACS Buffer (1x PBS, 2% heat-inactivated fetal calf serum [HI-FCS, Atlanta biologicals]) for 30 min at 4ºC. Following blocking, cells were stained in FACS buffer with fluorochrome-conjugated antibodies in the dark for 30 min at 4ºC. Cells were then fixed in FACS Lysis Buffer (BD) per manufacturer's instructions and resuspended in PBS. For transcription factor staining, cells were fixed, permeabilized and stained using the Transcription Factor Staining Kit (eBioscience) per manufacturer's instructions. The following fluorochrome-conjugated antibodies were used: CD4 (clone GK1.5), CD8a (53-6.7), CD11a (M17/4), CD11b (M1/70), CD44 (IM7), CD45.2 (104), CD49d (R1-2), CD80 (16-10A1), CD86 (GL-1), CD90.1 (HIS51), CD90.2 (30-H12), CD95 (15A7), CD178 (MFL3), T-bet (4B10), Foxp3 (FJK16s), Ly6G (1A8), Ly6C (HK1.4 and AL-21), and I-A/I-E (M5/114.15.2) from Biolegend; CD4 (RM4-5) from eBioscience; and Siglec F (E40-2440) and CD11c (HL3) from BD Biosciences. For some experiments a fixable viability dye (eBioscience, cat#65-0865) and Annexin V (eBioscience, cat#BMS306APC-20) were used according to manufacturer's instructions. For detection of active Caspases, Vybrant FAM Caspase-3/7 and Caspase-8 Assay kits (ThermoFisher Scientific, cat#V35118 and V35119) were used according to manufacturer's instructions. Data was acquired on a BD LSR II and analyzed with FlowJo software (FlowJo, LLC). Live cells were sorted for in vitro culture experiments on a BD FACS Aria II.

DC–T cell co-culture. This assay was adapted from a previously described assay (15). Live CD11b$^{hi/low/-}$ DCs (CD11c$^+$Siglec F$^-$) and IAV-specific CD4 T cells (CD90.2$^+$CD4$^+$CD49d$^+$CD11a$^+$) were stained and sorted from lungs or spleens of mice seven days post-infection as above. 1x10^4 DCs and 1x10^4 IAV-specific CD4 T cells or 2x10^4 CD4 T cells alone per well of a 96-well plate were incubated in Iscove's DMEM (Gibco) containing 10% HI-FCS (Atlanta Biologicals), 1X β-mercaptoethanol (Gibco), 1X Penicillin/Streptomycin (Gibco), 1X L-glutamine (Gibco), and 1X sodium pyruvate (Gibco). For some experiments, 2.5µg/mL Fas-Fc (R&D systems) was included. Cells were incubated for 12 hrs at 37ºC, 5% CO$_2$, and then assessed by flow cytometry as above.

Isolation of CD4 T cells. For adoptive transfer experiments, splenic naïve CD4 T cells were purified by magnetic separation using a negative selection kit (Stemcell Technologies). Purified cells were suspended in sterile DMEM and 1×10^5 WT and 1×10^5 *Nlrc4$^{-/-}$* cells were injected intravenously 24 hrs prior to IAV infection.

Western Blotting. Lysates were prepared in Radio Immunoprecipitation Assay (RIPA) buffer (Cell Signaling Technologies) with 1mM PMSF per manufacturer's instructions. Lungs were homogenized in RIPA buffer using a Tissue-Tearor (BioSpec Products). A BCA Assay (ThermoFisher Scientific) was performed to measure total protein in lung homogenates, then samples were diluted to the same concentration in RIPA buffer. Lysates were stored at -80ºC. Proteins were separated on a NuPAGE gel (Invitrogen) and transferred to a PVDF membrane using the XCell II blotting system (Invitrogen). Membranes were blocked with 5% nonfat milk or BSA and incubated with antibody against Caspase-1 p20 (1:1000, AG-20B-0042-C100, Adipogen), β-actin (1:2000, sc-47778, Santa Cruz Biotechnology), Phospho-Akt1 (1:1000, CST#9018, Cell Signaling Technology), Akt1 (1:1000, CST#75692, Cell Signaling Technology), Phospho-FoxO3a (1:1000, CST#9466) or FoxO3a (1:1000, CST#12829, Cell Signaling Technology) overnight at 4ºC. Following washing, membranes were incubated with HRP-tagged anti-mouse IgG (1706516, Bio-Rad) or anti-rabbit IgG (NA934, GE Healthcare) and developed using SuperSignal West Pico or Femto substrate (Thermo Fisher Scientific).

Real-time PCR. Total RNA was isolated from BMDC using RNeasy Mini Kit (Qiagen), and cDNA was generated with PrimeScript RT Master Mix (Takara Bio USA) according to the manufacturer's instructions. Real-time PCR was carried out using CFX Real-Time PCR System (Bio-Rad) with SYBR Green molecular probe (Applied Biosystems). The levels of mRNA were quantitatively analyzed by Bio-Rad CFX Manager 3.1 software. Relative mRNA expression level was

normalized by the housekeeping gene β-actin. The primers used for FasL, forward primer 5'-CCTGTGTCACCACTACCACC-3', reverse primer 5'-CCACCGGTAGCCACAGATTT-3'; for β-Actin, forward primer 5'-CGAGGTATCCTGACCCTGAA-3' and reverse primer 5'-GGTGTGGTGCCAGATCTTCT-3'.

DC adoptive transfer. Bone marrow-derived dendritic cells (BMDCs) were differentiated as previously described (54). BMDCs were analyzed by flow cytometry and/or $5x10^5$ BMDCs in 50µL sterile DMEM were administered intranasally to IAV-infected mice five days post-infection.

Statistics. Data were graphed and indicated statistical tests performed using GraphPad Prism software (GraphPad Software). A p value less than 0.05 was considered significant.

Study Approval. All animal studies were approved by and performed according to the guidelines of the Institutional Animal Care and Use Committee at the University of Iowa and Cedars-Sinai Medical Center.

Author contributions
EEH, FSS and SLC conceptualized the project. EEH, KLL, FSS and SLC developed the methodology. EEH and JD performed the experiments with assistance and/or reagents from ZRZ, AMM, RAL and KLL. EEH, JD, FSS and SLC performed formal analysis. EEH, FSS and SLC wrote the original draft. EEH, JD, ZRZ, AMM, KLL, GAB, PC, FSS and SLC reviewed and edited the manuscript. FSS and SLC acquired funding. GAB, FSS and SLC supervised the project.

References

1.	Thompson WW, Shay DK, Weintraub E, and et al. Influenza-associated hospitalizations in the united states. *JAMA.* 2004;292(11):1333-40.
2.	Wilkinson TM, Li CK, Chui CS, Huang AK, Perkins M, Liebner JC, et al. Preexisting influenza-specific CD4+ T cells correlate with disease protection against influenza challenge in humans. *Nat Med.* 2012;18(2):274-80.
3.	Sridhar S, Begom S, Bermingham A, Hoschler K, Adamson W, Carman W, et al. Cellular immune correlates of protection against symptomatic pandemic influenza. *Nat Med.* 2013;19(10):1305-12.
4.	Topham DJ, Tripp RA, and Doherty PC. CD8+ T cells clear influenza virus by perforin or Fas-dependent processes. *J Immunol.* 1997;159(11):5197-200.
5.	Brincks EL, Katewa A, Kucaba TA, Griffith TS, and Legge KL. CD8 T cells utilize TRAIL to control influenza virus infection. *J Immunol.* 2008;181(7):4918-25.
6.	Sun J, and Braciale TJ. Role of T cell immunity in recovery from influenza virus infection. *Curr Opin Virol.* 2013;3(4):425-9.
7.	Brown DM, Lee S, Garcia-Hernandez Mde L, and Swain SL. Multifunctional CD4 cells expressing gamma interferon and perforin mediate protection against lethal influenza virus infection. *J Virol.* 2012;86(12):6792-803.
8.	Cardani A, Boulton A, Kim TS, and Braciale TJ. Alveolar Macrophages Prevent Lethal Influenza Pneumonia By Inhibiting Infection Of Type-1 Alveolar Epithelial Cells. *PLoS Pathog.* 2017;13(1):e1006140.
9.	Brandes M, Klauschen F, Kuchen S, and Germain Ronald N. A Systems Analysis Identifies a Feedforward Inflammatory Circuit Leading to Lethal Influenza Infection. *Cell.* 2013;154(1):197-212.
10.	Antunes I, and Kassiotis G. Suppression of innate immune pathology by regulatory T cells during Influenza A virus infection of immunodeficient mice. *J Virol.* 2010;84(24):12564-75.
11.	Mock JR, Garibaldi BT, Aggarwal NR, Jenkins J, Limjunyawong N, Singer BD, et al. Foxp3 regulatory T cells promote lung epithelial proliferation. *Mucosal Immunol.* 2014.

12. Hemann EA, and Legge KL. Peripheral regulation of T cells by dendritic cells during infection. *Immunol Res.* 2014.

13. McGill J, Van Rooijen N, and Legge KL. IL-15 trans-presentation by pulmonary dendritic cells promotes effector CD8 T cell survival during influenza virus infection. *J Exp Med.* 2010;207(3):521-34.

14. McGill J, Van Rooijen N, and Legge KL. Protective influenza-specific CD8 T cell responses require interactions with dendritic cells in the lungs. *J Exp Med.* 2008;205(7):1635-46.

15. Langlois RA, and Legge KL. Plasmacytoid dendritic cells enhance mortality during lethal influenza infections by eliminating virus-specific CD8 T cells. *J Immunol.* 2010;184(8):4440-6.

16. Legge KL, and Braciale TJ. Lymph node dendritic cells control CD8+ T cell responses through regulated FasL expression. *Immunity.* 2005;23(6):649-59.

17. Boonnak K, Vogel L, Feldmann F, Feldmann H, Legge KL, and Subbarao K. Lymphopenia associated with highly virulent H5N1 virus infection due to plasmacytoid dendritic cell-mediated apoptosis of T cells. *J Immunol.* 2014;192(12):5906-12.

18. Zhao Y, and Shao F. The NAIP-NLRC4 inflammasome in innate immune detection of bacterial flagellin and type III secretion apparatus. *Immunol Rev.* 2015;265(1):85-102.

19. Kupz A, Guarda G, Gebhardt T, Sander LE, Short KR, Diavatopoulos DA, et al. NLRC4 inflammasomes in dendritic cells regulate noncognate effector function by memory CD8+ T cells. *Nat Immunol.* 2012;13:162.

20. Janowski AM, Colegio OR, Hornick EE, McNiff JM, Martin MD, Badovinac VP, et al. NLRC4 suppresses melanoma tumor progression independently of inflammasome activation. *J Clin Invest.* 2016;126(10):3917-28.

21. Allen IC, Scull MA, Moore CB, Holl EK, McElvania-TeKippe E, Taxman DJ, et al. The NLRP3 inflammasome mediates in vivo innate immunity to influenza A virus through recognition of viral RNA. *Immunity.* 2009;30(4):556-65.

22. Thomas PG, Dash P, Aldridge JR, Jr., Ellebedy AH, Reynolds C, Funk AJ, et al. The intracellular sensor NLRP3 mediates key innate and healing responses to influenza A virus via the regulation of caspase-1. *Immunity.* 2009;30(4):566-75.

23. Tenthorey JL, Haloupek N, Lopez-Blanco JR, Grob P, Adamson E, Hartenian E, et al. The structural basis of flagellin detection by NAIP5: A strategy to limit pathogen immune evasion. *Science.* 2017;358(6365):888-93.

24. Poyet JL, Srinivasula SM, Tnani M, Razmara M, Fernandes-Alnemri T, and Alnemri ES. Identification of Ipaf, a human caspase-1-activating protein related to Apaf-1. *J Biol Chem.* 2001;276(30):28309-13.

25. Tumpey TM, Garcia-Sastre A, Taubenberger JK, Palese P, Swayne DE, Pantin-Jackwood MJ, et al. Pathogenicity of influenza viruses with genes from the 1918 pandemic virus: functional roles of alveolar macrophages

and neutrophils in limiting virus replication and mortality in mice. *J Virol.* 2005;79(23):14933-44.

26. Ramos I, and Fernandez-Sesma A. Modulating the Innate Immune Response to Influenza A Virus: Potential Therapeutic Use of Anti-Inflammatory Drugs. *Front Immunol.* 2015;6:361.

27. Richards KA, Chaves FA, Krafcik FR, Topham DJ, Lazarski CA, and Sant AJ. Direct ex vivo analyses of HLA-DR1 transgenic mice reveal an exceptionally broad pattern of immunodominance in the primary HLA-DR1-restricted CD4 T-cell response to influenza virus hemagglutinin. *J Virol.* 2007;81(14):7608-19.

28. Sant AJ, Chaves FA, Krafcik FR, Lazarski CA, Menges P, Richards K, et al. Immunodominance in CD4 T-cell responses: implications for immune responses to influenza virus and for vaccine design. *Expert review of vaccines.* 2007;6(3):357-68.

29. Crowe SR, Miller SC, Brown DM, Adams PS, Dutton RW, Harmsen AG, et al. Uneven distribution of MHC class II epitopes within the influenza virus. *Vaccine.* 2006;24(4):457-67.

30. McDermott DS, and Varga SM. Quantifying antigen-specific CD4 T cells during a viral infection: CD4 T cell responses are larger than we think. *J Immunol.* 2011;187(11):5568-76.

31. Hornick EE, Banoth B, Miller AM, Zacharias ZR, Jain N, Wilson ME, et al. Nlrp12 Mediates Adverse Neutrophil Recruitment during Influenza Virus Infection. *J Immunol.* 2018;200(3):1188-97.

32. Brown DM, Roman E, and Swain SL. CD4 T cell responses to influenza infection. *Semin Immunol.* 2004;16(3):171-7.

33. Leon B, Bradley JE, Lund FE, Randall TD, and Ballesteros-Tato A. FoxP3+ regulatory T cells promote influenza-specific Tfh responses by controlling IL-2 availability. *Nature communications.* 2014;5:3495.

34. Tripp RA, Sarawar SR, and Doherty PC. Characteristics of the influenza virus-specific CD8+ T cell response in mice homozygous for disruption of the H-2lAb gene. *J Immunol.* 1995;155(6):2955-9.

35. Sant AJ, Richards KA, and Nayak J. Distinct and complementary roles of CD4 T cells in protective immunity to influenza virus. *Curr Opin Immunol.* 2018;53:13-21.

36. Legge KL, and Braciale TJ. Accelerated migration of respiratory dendritic cells to the regional lymph nodes is limited to the early phase of pulmonary infection. *Immunity.* 2003;18(2):265-77.

37. Latchman Y, Wood CR, Chernova T, Chaudhary D, Borde M, Chernova I, et al. PD-L2 is a second ligand for PD-1 and inhibits T cell activation. *Nat Immunol.* 2001;2(3):261-8.

38. Suss G, and Shortman K. A subclass of dendritic cells kills CD4 T cells via Fas/Fas-ligand-induced apoptosis. *J Exp Med.* 1996;183(4):1789-96.

39. Mariathasan S, Newton K, Monack DM, Vucic D, French DM, Lee WP, et al. Differential activation of the inflammasome by caspase-1 adaptors ASC and Ipaf. *Nature.* 2004;430(6996):213-8.

40. Brunet A, Bonni A, Zigmond MJ, Lin MZ, Juo P, Hu LS, et al. Akt promotes cell survival by phosphorylating and inhibiting a Forkhead transcription factor. *Cell.* 1999;96(6):857-68.

41. Zhang H, Luo J, Alcorn JF, Chen K, Fan S, Pilewski J, et al. AIM2 Inflammasome Is Critical for Influenza-Induced Lung Injury and Mortality. *J Immunol.* 2017;198(11):4383.

42. Eisfeld AJ, Gasper DJ, Suresh M, and Kawaoka Y. C57BL/6J and C57BL/6NJ Mice Are Differentially Susceptible to Inflammation-Associated Disease Caused by Influenza A Virus. *Front Microbiol.* 2018;9:3307.

43. Vanden Berghe T, Hulpiau P, Martens L, Vandenbroucke RE, Van Wonterghem E, Perry SW, et al. Passenger Mutations Confound Interpretation of All Genetically Modified Congenic Mice. *Immunity.* 2015;43(1):200-9.

44. Ulland TK, Jain N, Hornick EE, Elliott EI, Clay GM, Sadler JJ, et al. Nlrp12 mutation causes C57BL/6J strain-specific defect in neutrophil recruitment. *Nat Commun.* 2016;7:13180.

45. Yamamoto TN, Lee P-H, Vodnala SK, Gurusamy D, Kishton RJ, Yu Z, et al. T cells genetically engineered to overcome death signaling enhance adoptive cancer immunotherapy. *The Journal of Clinical Investigation.* 2019;129(4).

46. Kavurma MM, and Khachigian LM. Signaling and transcriptional control of Fas ligand gene expression. *Cell Death Differ.* 2003;10(1):36-44.

47. Manning BD, and Toker A. AKT/PKB Signaling: Navigating the Network. *Cell.* 2017;169(3):381-405.

48. Lara-Tejero M, Sutterwala FS, Ogura Y, Grant EP, Bertin J, Coyle AJ, et al. Role of the caspase-1 inflammasome in Salmonella typhimurium pathogenesis. *J Exp Med.* 2006;203(6):1407-12.

49. Sutterwala FS, Ogura Y, Szczepanik M, Lara-Tejero M, Lichtenberger GS, Grant EP, et al. Critical role for NALP3/CIAS1/Cryopyrin in innate and adaptive immunity through its regulation of caspase-1. *Immunity.* 2006;24(3):317-27.

50. Kuida K, Lippke JA, Ku G, Harding MW, Livingston DJ, Su MS, et al. Altered cytokine export and apoptosis in mice deficient in interleukin-1 beta converting enzyme. *Science.* 1995;267(5206):2000-3.

51. Hoffmann E, Neumann G, Kawaoka Y, Hobom G, and Webster RG. A DNA transfection system for generation of influenza A virus from eight plasmids. *Proc Natl Acad Sci U S A.* 2000;97(11):6108-13.

52. Heaton NS, Sachs D, Chen CJ, Hai R, and Palese P. Genome-wide mutagenesis of influenza virus reveals unique plasticity of the hemagglutinin and NS1 proteins. *Proc Natl Acad Sci U S A.* 2013;110(50):20248-53.

53. Szretter KJ, Balish AL, and Katz JM. Influenza: propagation, quantification, and storage. *Curr Protoc Microbiol.* 2006;3(1):15G. 1.1-G. 1.22.

54. Helft J, Bottcher J, Chakravarty P, Zelenay S, Huotari J, Schraml BU, et al. GM-CSF Mouse Bone Marrow Cultures Comprise a Heterogeneous

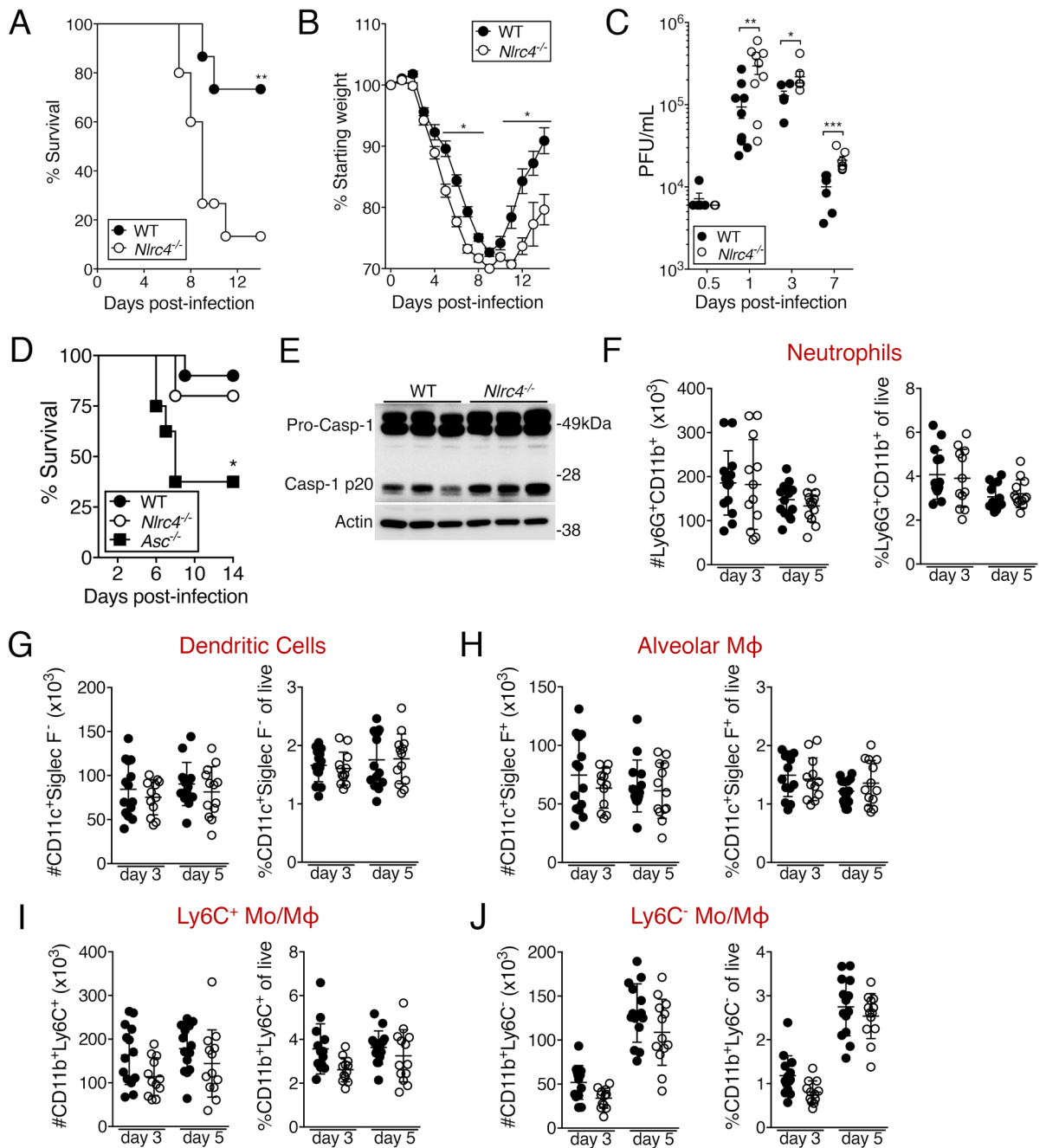Population of CD11c(+)MHCII(+) Macrophages and Dendritic Cells. *Immunity.* 2015;42(6):1197-211.

Figure 1. *Nlrc4*^{-/-} mice have reduced survival and viral clearance during IAV infection. (A-E) Mice were infected with a 0.5LD$_{50}$ (A-C, E) or 0.25LD$_{50}$ (D) inoculum of IAV. Mortality (A, D) and weight loss (B) were monitored, and pulmonary viral titers (C) were quantified by plaque assay at the indicated times post-infection. (E) Caspase-1 cleavage was assessed in lungs 24 hrs post-infection with IAV. Each lane represents one mouse. (F-J) Innate immune cells in the lungs were quantified at the indicated times post-infection. In addition to the markers shown, dead cells and doublets were excluded, then cells were gated on CD45.2 expression. Data are from one (E, n=3 per group and D, n=8-10 per group), or pooled from two (A, B, n=14 per group and C, n=5=9 per group) or three (F-J, n=12-14 per group) separate experiments. *p<0.05, **p<0.01, ***p<0.001, Mantel-Cox Test (A, D), one-way ANOVA with Tukey's post-hoc analysis (B), two-tailed Student's t-test (C).
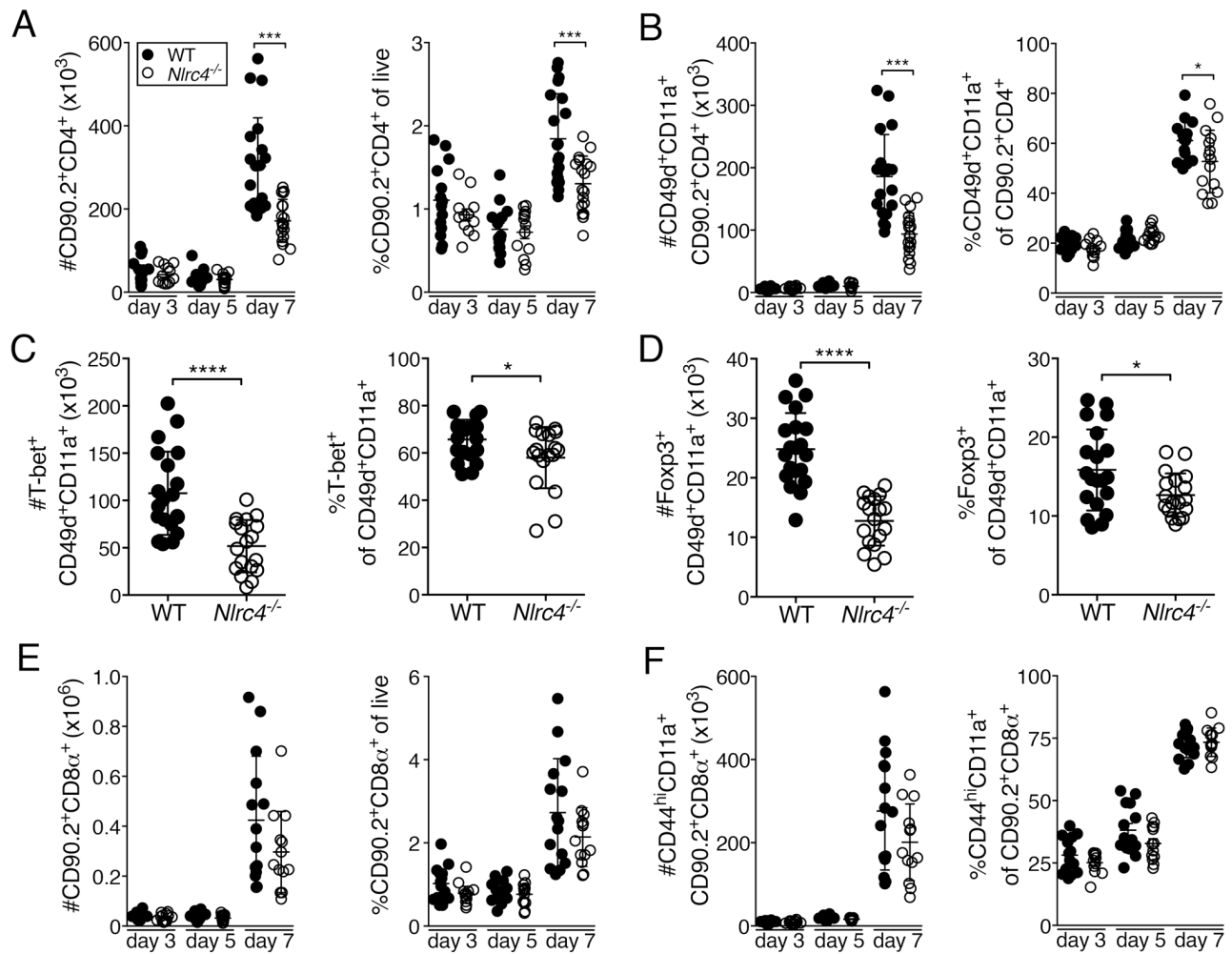
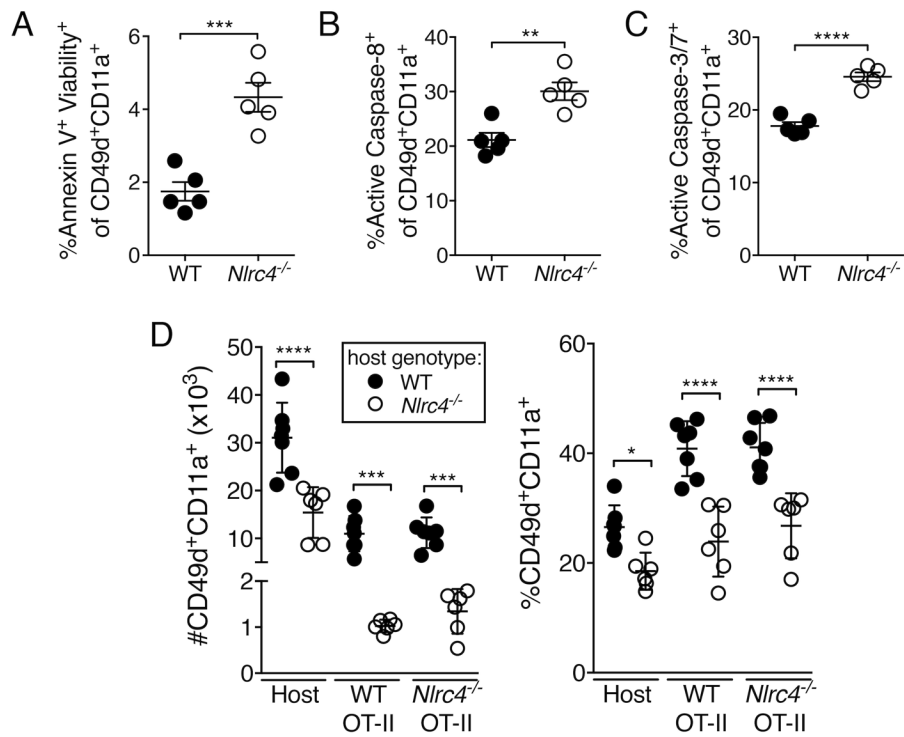Figure 2. Decreased IAV-specific CD4 T cells in the lungs of *Nlrc4*^{-/-} mice seven days post-infection. (A-F) Mice were infected with a $0.5LD_{50}$ inoculum of IAV and lung CD4 T cell subsets were enumerated by flow cytometry at the indicated time (A, B, E, F) or day seven post-infection (C, D). Data are from three (C, D, n=12-16 per group) or four (A, B, E, F, n=13-20 per group) independent experiments, error bars represent SEM. *p<0.05, **p<0.01, ***p<0.001, ****p<0.0001, two-tailed Student's t-test.

Figure 3. Increased death of IAV-specific CD4 T cells in the lungs of *Nlrc4*^{-/-} mice at seven days post-infection. (A-C) Mice were infected with a $0.5LD_{50}$ inoculum of IAV and cells staining positive for the indicated markers/dyes were enumerated in the lungs at day seven post-infection by flow cytometry. (D) CD90.2$^+$ WT and *Nlrc4*$^{-/-}$ hosts received 1×10^5 naïve CD90.1/2$^+$ WT and 1×10^5 CD90.1$^+$ *Nlrc4*$^{-/-}$ OT-II cells i.v., followed one day later by infection with a $0.5LD_{50}$ inoculum of IAV expressing Ova$_{323-339}$. Seven days post-infection the indicated cells were quantified in the lungs. Data are representative of two independent experiments, n=5-6 per group, error bars represent SEM. *p<0.05, **p<0.01, ***p<0.001, ****p<0.0001, two-tailed Student's t-test.
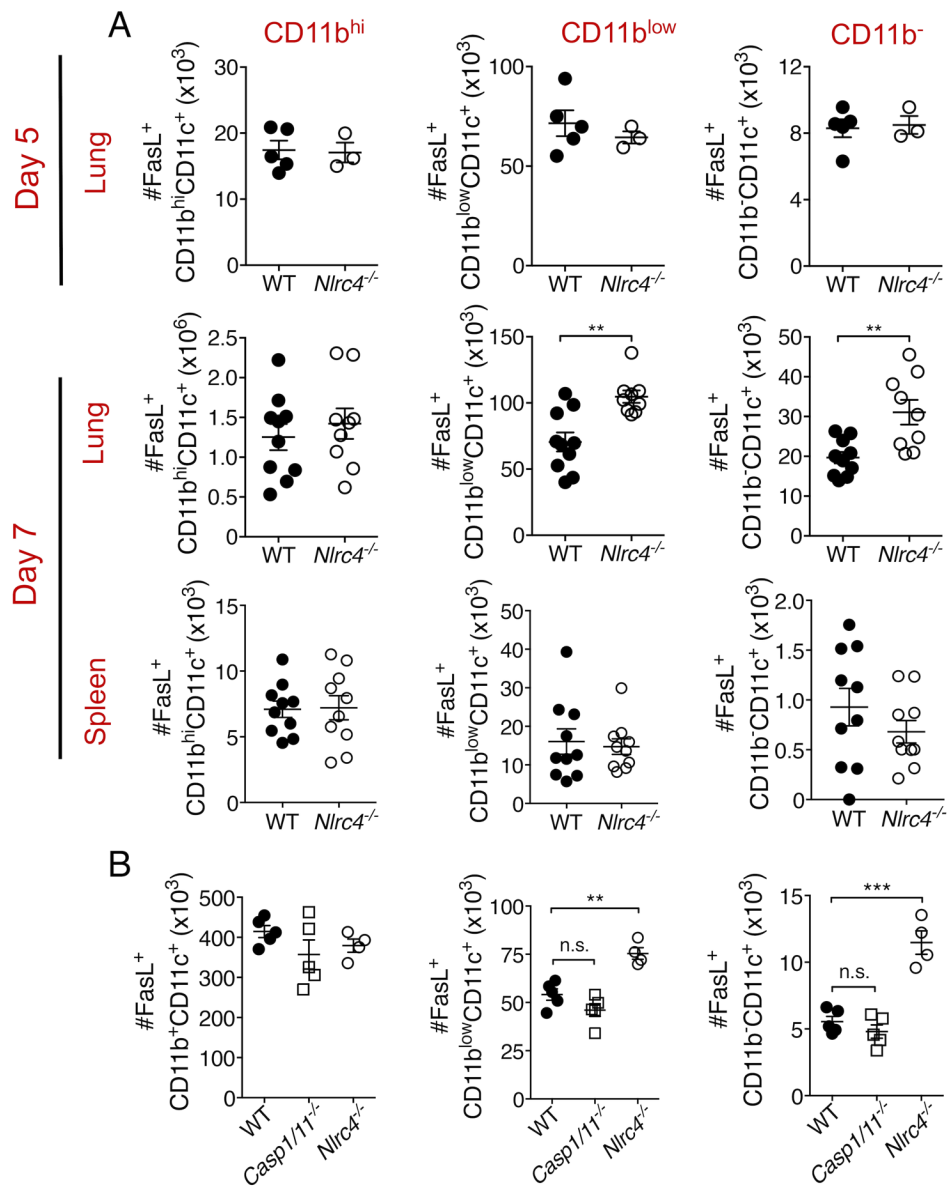
Figure 4. Increased FasL+ DCs in the lungs of *Nlrc4-/-* mice during IAV infection. (A, B) Mice were infected with a 0.5LD$_{50}$ IAV and FasL+ DCs were enumerated by flow cytometry in the indicated organ and time post-infection (A) or in the lung at day seven post-infection (B). Data are from one (A, day 5, and B, n=3-5 per group) or two (A, day 7, n=9-10 per group) separate experiments, error bars represent SEM. **p<0.01; ****p<0.0001 two-tailed Student's t-test.
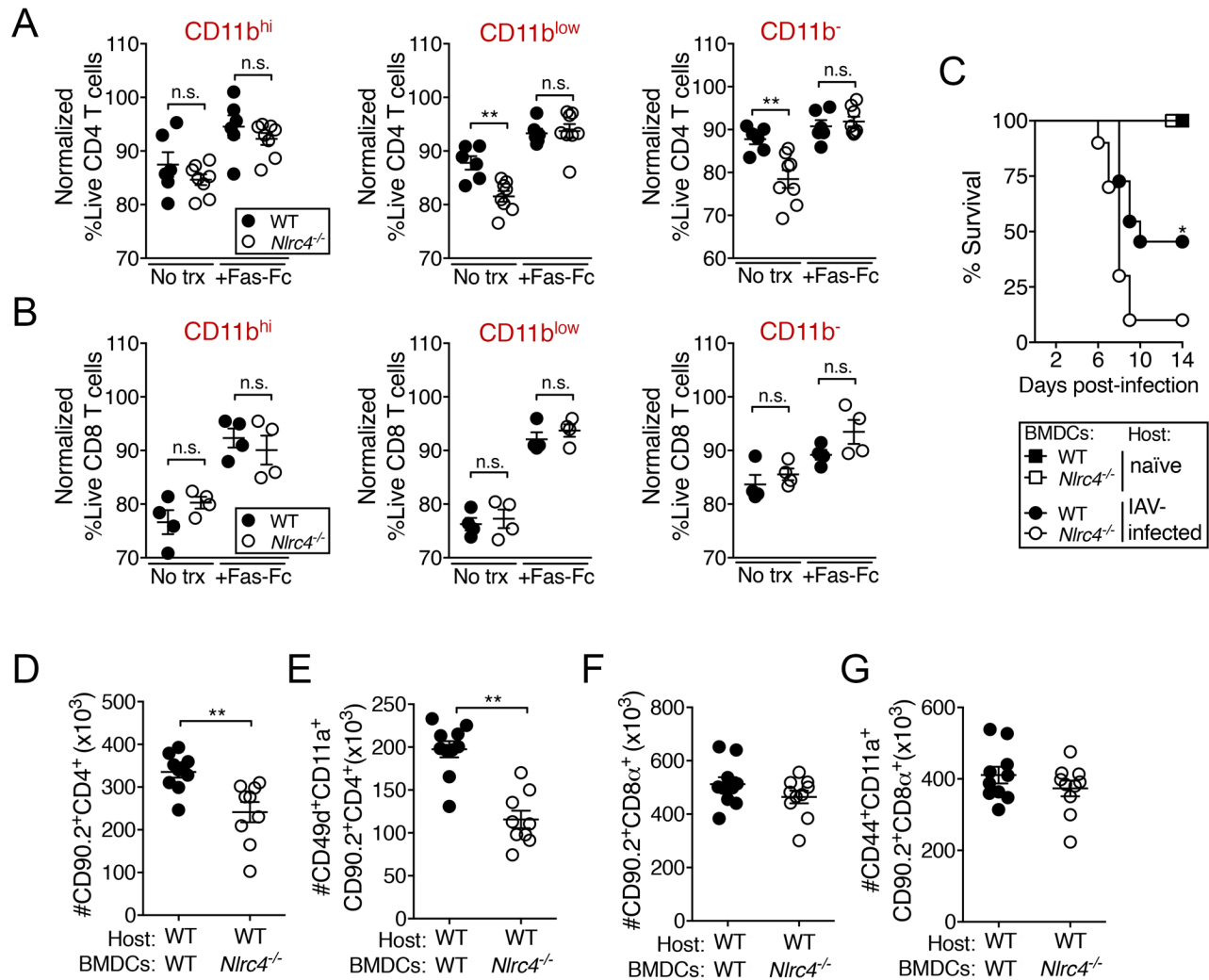
Figure 5. Increased FasL-mediated killing of CD4, but not CD8, T cells by $Nlrc4^{-/-}$ DCs during IAV infection. Mice were infected with a $0.5LD_{50}$ IAV or left uninfected (naïve). (A, B) Pulmonary DCs and T cells were purified at seven days post-infection. Pooled WT+$Nlrc4^{-/-}$ T cells were incubated with the indicated populations of DCs for 12hrs with (+Fas-Fc) or without (No trx) 2.5µg/mL Fas-Fc. Live CD4 and CD8 T cells (Annexin V⁻ Viability Dye⁻) were enumerated by flow cytometry. The proportion of live CD4 and CD8 T cells co-cultured with DCs was normalized to CD4 and CD8 T cells cultured alone. (C-G) At 5 days post-infection, WT mice received $5x10^5$ WT or $Nlrc4^{-/-}$ BMDC intranasally and survival assessed (C). Pulmonary CD4 and CD8 T cells were quantified at seven days post-infection (C-G). Data are from one (B, n=4 per group) or two (A, n=8 per group, and C-G, n=10 per group) separate experiments, error bars represent SEM. *p<0.05, **p<0.01; two-tailed Student's t-test (A, D, E), Mantel-Cox test (C).
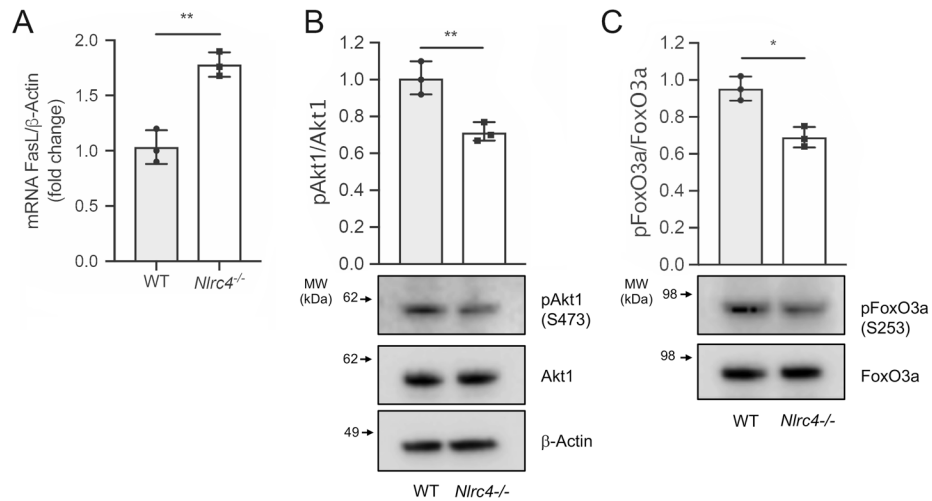
Figure 6. NLRC4 regulates FasL expression at the transcriptional level in BMDC. (A) *Fasl* mRNA expression was assessed in WT and *Nlrc4⁻/⁻* BMDC by qPCR and normalized to β-actin. (B, C) pAkt1 and pFoxO3a protein levels in whole cell lysates of BMDC from WT and *Nlrc4⁻/⁻* mice were analyzed by immunoblot. Densitometric analysis was performed with Bio-Rad Image Lab software (ver.5.2.1). Total FoxO3a, Akt1 and β-actin were used as loading controls. Data are pooled from three independent experiments. *p<0.05, **p<0.01, two-tailed Student's t-test.